Research Article

Journal of PeptideScience

Received: 16 January 2009 Revised: 6 August 2009 Accepted: 6 August 2009 Published online in Wiley Interscience: 14 October 2009

(www.interscience.com) DOI 10.1002/psc.1184

Minimal motif peptide structure of metzincin clan zinc peptidases in micelles

Akira Onoda, Takako Suzuki, Hiroaki Ishizuka, Rumiko Sugiyama, Shinya Ariyasu and Takeshi Yamamura*

It is well known that the functions of metalloproteins generally originate from their metal-binding motifs. However, the intrinsic nature of individual motifs remains unknown, particularly the details about metal-binding effects on the folding of motifs; the converse is also unknown, although there is no doubt that the motif is the core of the reactivity for each metalloprotein. In this study, we focused our attention on the zinc-binding motif of the metzincin clan family, HEXXHXXGXXH; this family contains the general zinc-binding sequence His–Glu–Xaa–Xaa–His (HEXXH) and the extended GXXH region. We adopted the motif sequence of stromelysin-1 and investigated the folding properties of the Trp-labeled peptides WAHEIAHSLGLFHA (STR-W1), AWHEIAHSLGLFHA (STR-W2), AHEIAHSLGWFHA (STR-W11), and AHEIAHSLGLFHWA (STR-W14) in the presence and absence of zinc ions in hydrophobic micellar environments by circular dichroism (CD) measurements. We accessed successful incorporation of these zinc peptides into micelles using quenching of Trp fluorescence. Results of CD studies indicated that two of the Trp-incorporated peptides, STR-W1 and STR-W14, exhibited helical folding in the hydrophobic region of cetyltrimethylammonium chloride micelle. The NMR structural analysis of the apo STR-W14 revealed that the conformation in the *C*-terminus GXXH region significantly differred between the apo state in the micelle and the reported Zn-bound state of stromelysin-1 in crystal structures. The structural analyses of the qualitative Zn-binding properties of this motif peptide provide an interesting Zn-binding mechanism: the minimum consensus motif in the metzincin clan, a basic zinc-binding motif with an extended GXXH region, has the potential to serve as a preorganized Zn binding scaffold in a hydrophobic environment.

Supporting information may be found in the online version of this article

Keywords: zinc peptidase; minimal peptide; NMR structure; zinc binding; folding

Introduction

It is well known that a variety of metal-binding motifs is conserved in metal proteins and that functions of metalloproteins generally originate from their metal-binding motifs. These motifs are of considerable interest because the intrinsic nature of individual motifs in the presence or absence of metal ions is almost unknown, particularly the details about metal-binding effects on the folding of motifs; the converse is also unknown. Acquiring knowledge on the motifs will lead to the understanding of the primitive role of these motifs. Among the metal-binding motifs, motifs that contain cysteine (Cys) residues are the ones mainly investigated because of the stability of M-Cys bonds, where M denotes biologically active metals such as iron (Fe), nickel (Ni), and zinc (Zn) [1–4].

Zn is a biologically important metal ion that plays catalytic roles and/or works as a structural cofactor. A variety of Zn-binding motifs conserved in zinc proteins are also known. The best known Zn-binding motif is the classical Cys_2His_2 Zn finger motif that possesses the general sequence (Phe, Tyr)–X–Cys–X_{2-4}–Cys–X_3–Phe–X_5–Leu–X_2–His–$X_{3,4}$–His–X_{2-6}, where X is any amino acid. Each unit binds a single Zn ion (Zn^{2+}) forming the a stable and common $\beta\beta\alpha$ folding structure by Zn coordination [5]. Results of biophysical studies on Zn finger peptides have provided insights into some of the central questions for protein folding; metal-binding by Zn finger peptides appears to involve a transition from an unfolded apoprotein to a well-folded metalloprotein [6, 7].

However, there have been no reports on the combination of Zn and motifs that lack Cys as a coordination site for Zn. The Zn coordination with His, Glu, or Asp residue are weakly stabilized in comparison with Zn–Cys; therefore, it is interesting to note whether or not such a motif reproduces the folding of the active center of the native protein in the absence of Zn and other parts of the protein – in other words, whether the motif itself provides the pocket for Zn coordination. Therefore, we were motivated to investigate the intrinsic nature of the smallest His – only motif as our starting point. In this study, we focused our attention on the Zn-binding motif of the metzincin clan family, HEXXHXXGXXH; this family contains the general Zn-binding sequence His–Glu–Xaa–Xaa–His (HEXXH) and the extended GXXH region.

In a considerable number of metallopeptidases, the HEXXH fragment is highly conserved in the zinc active site [8,9]. Crystal

* *Correspondence to: Takeshi Yamamura, Faculty of Science, Department of Chemistry, Tokyo University of Science, Kagurazaka 1-3, Shinjuku-ku, Tokyo 162-8601, Japan. E-mail: tyamamur.tus@gmail.com*

Faculty of Science, Department of Chemistry, Tokyo University of Science, Kagurazaka 1-3, Shinjuku-ku, Tokyo 162-8601, Japan

Journal of PeptideScience

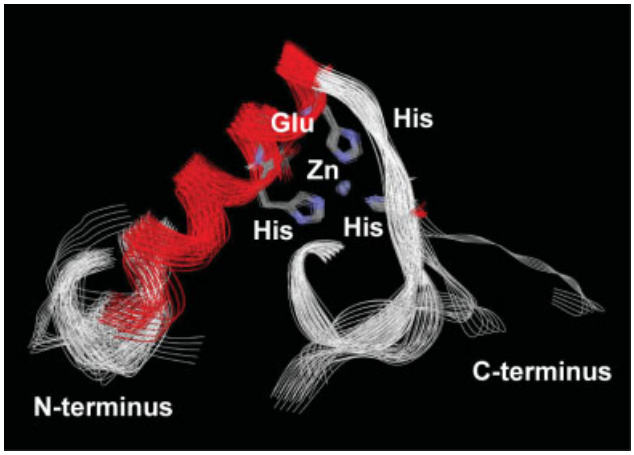

Figure 1. The local structures containing the motif parts of endopeptidase, His(i)-Glu(i + 1)-X2- His(i + 4)-X2-Gly-X2-His(i + 10)/Zn^{2+}, that belong to metzincin clan are shown. Twenty-seven units obtained from PDB structures (1b8y, 1bkc, 1bsw, 1bud, 1cge, 1cqr, 1dth, 1fbl, 1hfc, 1htd, 1iaf, 1kbc, 1mmb, 1mmp, 1mmq, 1mnc, 1qib, 1sat, 1slm, 1srp, 1uea, 3aig, 4aig, 456c, 830c, 966c, and 1bqo) are superimposed at the main chain Cα atoms of the motif (RMSD = 0.12715–0.34923 Å).

STR-W1	WAHEIAHSLGLFHA
STR-W2	AWHEIAHSLGLFHA
STR-W11	AHEIAHSLGWFHA
STR-W14	AHEIAHSLGLFHWA

Scheme 1. Amino acid sequences of Trp-labeled motif peptides used in this study.

structural analyses of thermolysin revealed that the HEXXH motif is included in an active site helix. The two His residues coordinate with Zn^{2+} in a protein, and the carboxyl side chain of the glutamate interacts with a Zn-bound water molecule. The HEXXH motif has been found not only in the thermolysin family but also in Zn peptidases [10]. Among the 30 families of Zn peptidases, four distinct families – astacins, adamalysins, serralysins, and matrix metalloproteinases [11] – are classified into the 'metzincin clan' [12] on the basis of the common topology of their primary structure having an elongated HEXXHXXGXXH motif as a Zn-binding active site [13]. Extensive X-ray structural analyses of all the proteins in this clan have shown that their HEXXHXXGXXH/Zn^{2+} fragment preserves a structural similarity characterized by a small helix and a $Zn(His)_3$ coordination unit linked to the conserved Glu residue via a water molecule (Figure 1) [11,14]. In this context, we previously investigated the structural features of the consensus sequence of the active sites of peptidases in the presence and absence of Zn^{2+} [15]. However, the peptide did not fold into a unique structure in aqueous media.

In this study, we adopted the motif sequence of stromelysin-1 and investigated the folding properties of micellar colloids in hydrophobic environments in the presence and absence of Zn^{2+}. Micellar colloids can provide hydrophobic environments in aqueous media, which helps in estimating the pH-dependent Zn-binding of peptides. Micelles or vesicles are generally used in the study of membrane proteins or membrane-interacting peptides [16–20]. In order to estimate the hydrophobicity of environments through fluorescence and quenching experiments, Trp was introduced for the structural study for tritrpticin [21]; thus, four Trp-labled peptides – WAHEIAHSLGLFHA (STR-W1), AWHEIAHSLGLFHA (STR-W2), AHEIAHSLGWFHA (STR-W11),

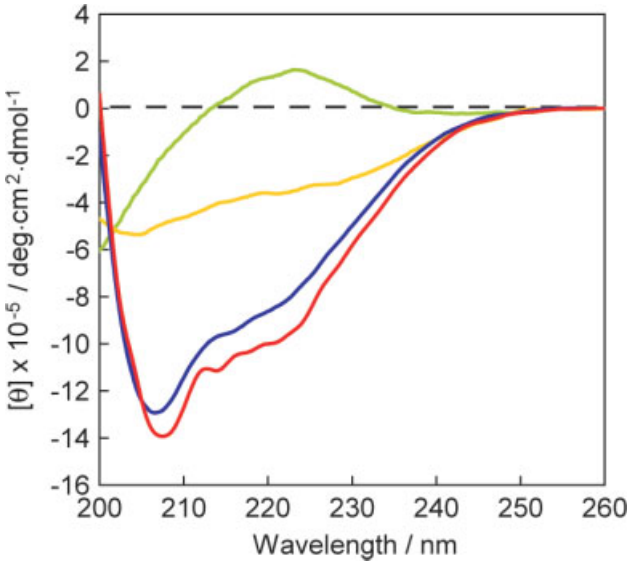

Figure 2. CD spectra of STR-W14 and STR-W14/Zn^{2+}. The apo peptide (green) and the Zn complex (yellow) in aqueous solution. The apo peptide (blue) and the Zn complex (red) in aqueous micellar solution; 100 μM peptide, 100 μM $Zn(ClO_4)_2$, and 10 mM CTAC, pH 7.

and AHEIAHSLGLFHWA (STR-W14) – were prepared in our study (Scheme 1). Trp is a weak α-helix former and a weak β-sheet former in the Chou–Fasman's prediction table [22]; therefore, its influence on the intrinsic folding of the motif was expected to be subordinate, except for the case of STR-W11. We found that these small fragments do not successfully fold in an aqueous solution, but fold in aqueous micellar solutions; this helps in estimating the pH-dependent Zn-binding of peptides through circular dichroism (CD), Trp fluorescence and quenching experiments. We also found that STR-W14 folds into a helix-containing structure in the absence of Zn^{2+} (NMR). The fragment binds Zn^{2+} into the micelle (mass spectrometry), which thereby slightly increases the helicity (CD).

Results and Discussion

Peptide Folding in Aqueous Micellar Solution

The folding nature of the STR model peptides was investigated by CD spectrophotometry. We found that both the apo and the Zn-bound peptides showed random coil structures in aqueous buffered solutions. In aqueous micellar solutions, both the apo and the Zn-bound peptides successfully folded. The CD profiles of STR-W14 peptide are shown in Figure 2. The characteristic negative band at 222 nm clearly indicates that STR-W14 and STR-W14/Zn^{2+} have helix conformations. The helicities of STR-W14 and STR-W14/Zn^{2+} were 27% and 32%, respectively, in the cethyltrimetylammonium chloride (CTAC) micelle. Therefore, the results suggest that the motif peptide has an inherent tendency to form helical parts due to hydrophobic circumstances. Polypeptides containing hydrophobic amino acids are known to have helical structures in hydrophobic environment, such as organic solvents and micelles.

To search for an appropriate type of micelles, we used four types of surfactants – CTAC, SDS, polyethyleneglycol laurylether (PGL), and dodecyl phosphatidyl choline (DPC) – as representatives of cationic, anionic, nonionic, and ampholytic surfactants, respectively. CD experiments for STR-W14 and its Zn complex

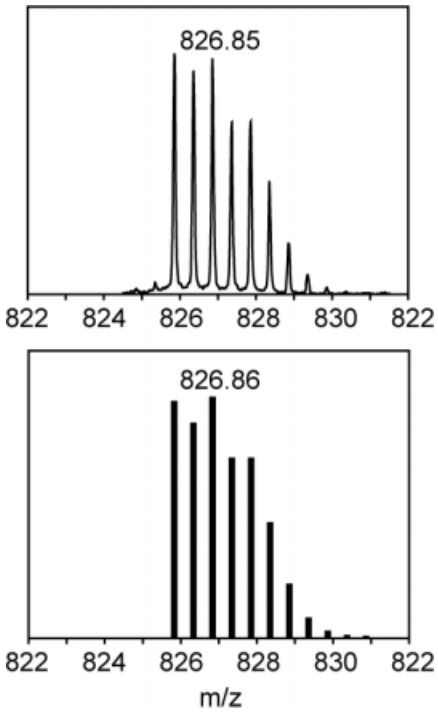

Figure 3. Observed and calculated signals of ESI-TOF MS (positive mode) of STR-W14/Zn^{2+} in aqueous micellar solution (100 μM peptide, 100 μM $Zn(ClO_4)_2$, 10 mM NH_4OAc buffer, pH 7, and 1 mM CTAC). Upper, observed; lower, calculated.

STR-W14/Zn^{2+} were performed in an aqueous micellar solution containing CTAC (10 mM), SDS (10 mM), PGL (0.5 mM), or DPC (10 mM); the results indicated that a relatively high peptide helicity can be achieved in the CTAC and DPC micellar solutions compared with the other two surfactants (see Supporting Information). Nonionic PGL is not suitable for burying the Zn peptide because its nonionic character excludes the charged complex. Anionic SDS is also inappropriate because Zn^{2+} is removed from the peptide complex by negatively charged sulfonate groups. Therefore, we selected the cationic CTAC micelle in the following experiments to promote successful helical folding of the peptide.

Zn Coordination to Motif Peptide

The formation of the peptide/Zn^{2+} complex was determined by ESI-TOF MS experiments. The observed spectrum of STR-W14/Zn^{2+} in the aqueous micellar solution was in good agreement with the calculated spectrum, as shown in Figure 3. The observed signal at 826.9 m/z was assigned to STR-W14 + Zn^{2+} while that at 826.3 was assigned to $C_{75}H_{105}N_{21}O_{18}Zn/2+$; the characteristic isotope pattern is in good agreement with the simulated spectrum. In the absence of micelles, the Zn-free peptides were also detected as a strong signal. On the other hand, the intensity for the Zn-bound form increased in the presence of the micelles under similar experimental conditions (Figure 4). Therefore, the MS analyses suggest that the peptide/Zn^{2+} complex is stabilized in the hydrophobic environment of the micelles.

Estimation of Hydrophobic Environment using Trp Fluorescence

To investigate the hydrophobic environment in which Trp-labeled motif peptides exist, we next measured the wavelength shift of

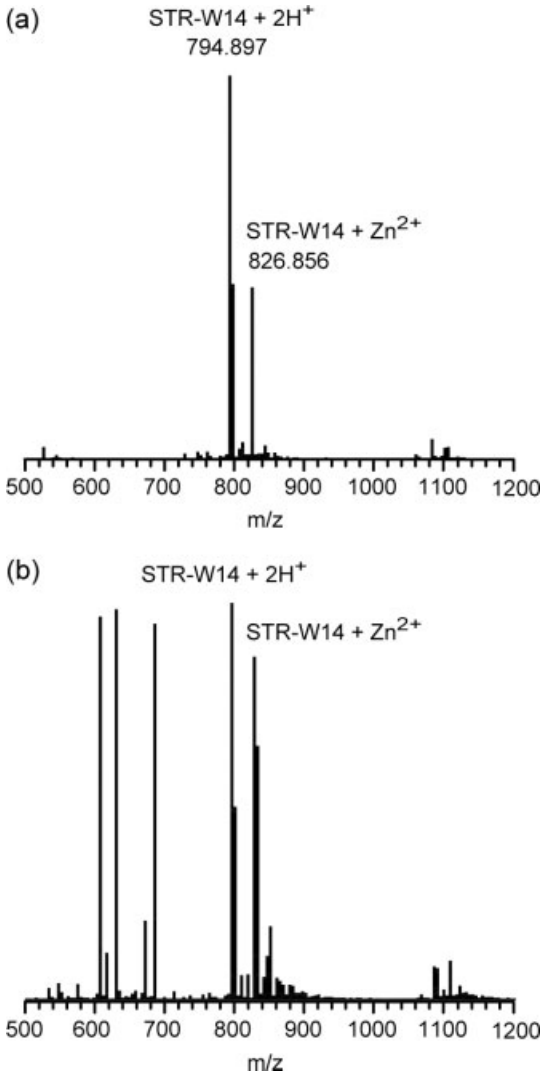

Figure 4. The results of ESI-TOF MS experiment (positive mode) for STR-W14/Zn^{2+} in (a) aqueous solution and (b) aqueous micellar solution (1 mM CTAC) are shown; 100 μM peptide, 100 μM $Zn(ClO_4)_2$, and 10 mM NH_4OAc buffer, pH 7.

Trp fluorescence as well as its quenching by acrylamide, which quantitatively indicates the accessibility of reagents to Trp [23]. The fluorescence spectra were shown in Figure 5 and the results are summarized in Table 1. The addition of CTAC to STR-W14 caused a 9-nm blue shift in the emission peak from 353 to 344 nm, and the fluorescence intensity increased from approximately 80 to 200 units. The blue shift and the increased intensity of Trp emissions indicate that the Trp in the CTAC micellar solution was located in an environment more hydrophobic than the aqueous solution. The other motif peptides also exhibited similar changes in the fluorescence spectra. Therefore, the Trp residues in both the free and the Zn forms were buried in the CTAC micelles.

As the other index of hydrophobicity, K_{SV} values were derived from the Stern–Volmer plot of acrylamide titration for each peptide and peptide complex. The data for STR-W14 is shown in Figure 6. We measured the K_{SV} of a protected Trp, Ac-Trp-OMe, as a standard to obtain $K_{SV} = 20.3$ and 15.4, which correspond to the presence and absence of the CTAC micelle, respectively. These values indicate that the Trp chromophore in the latter

Journal of PeptideScience

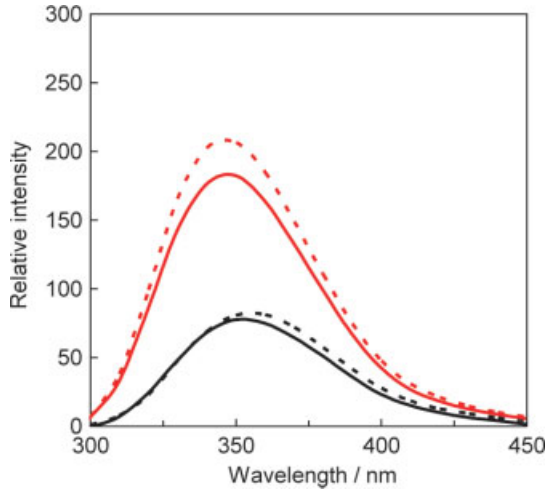

Figure 5. Fluorescence spectra (λex = 280 nm) of STR-W14 (dotted line) and STR-W14/Zn^{2+} (solid line). The spectra measured in aqueous solution and aqueous CTAC solution are in black and red line, respectively; 15 μM peptide, 15 μM $Zn(ClO_4)_2$, and 10 mM CTAC, pH 7.

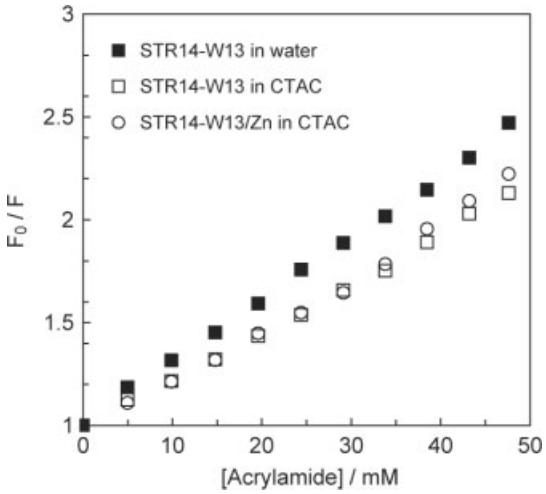

Figure 6. Stern–Volmer plots for STR-W14 were obtained by the sequential addition of small volumes of a fluorescence quencher, acrylamide (λex = 280 nm); 15 mM STR-W14, 15 mM $Zn(ClO_4)_2$, and 10 mM CTAC, pH 7.0.

Table 1. Em λ_{max} and K_{SV} values for Trp-labeled peptides

	Without micelle		In CTAC	
	Em λ_{max}/nm	K_{SV}/M^{-1}	Em λ_{max}/nm	K_{SV}/M^{-1}
STR-W1	353	20.9	345	23.4
STR-W1/Zn	356	–	348	27.9
STR-W2	351	19.0	338	20.4
STR-W2/Zn	343	–	339	25.9
STR-W11	354	18.5	345	22.9
STR-W11/Zn	353	–	342	20.1
STR-W14	353	30.2	344	22.6
STR-W14/Zn	357	–	345	22.2
Ac-Trp-OMe	357	20.3	344	15.4

solution is more protected from acrylamide quenching than in the former because of the incorporation of the chromophore into the hydrophobic region. Similarly, the remarkable decrease in K_{SV} from 30.2 to 22.6 M^{-1} in STR-W14 clearly supports the incorporation of this peptide into the micellar region, which is in accordance with steady-state fluorescence experiments. However, the other three peptides showed slightly increased K_{SV} values in the presence of the CTAC micelle. We speculate that these peptides aggregated in the aqueous solution to induce self-quenching. The results indicate that STR peptides and their Zn complexes are actually located in the inner region of the CTAC micelle.

The fluorescence spectra of Ac-Trp-OMe (15 μM) were measured in various media with different dipole moments and dielectricities, such as H_2O, MeOH, CH_3CN, DMSO, and toluene, to estimate the hydrophobicity of the Trp environment. A plot of the fluorescence intensity with solvent polarity parameters produced a linear relationship (see Supporting Information). This relationship indicates that the Trp environment in the micelles was similar to DMSO or MeOH. Therefore, the Trp residues of STR peptides are presumably located near the surface of the hydrophobic core of the micelles in the presence and absence of Zn^{2+}.

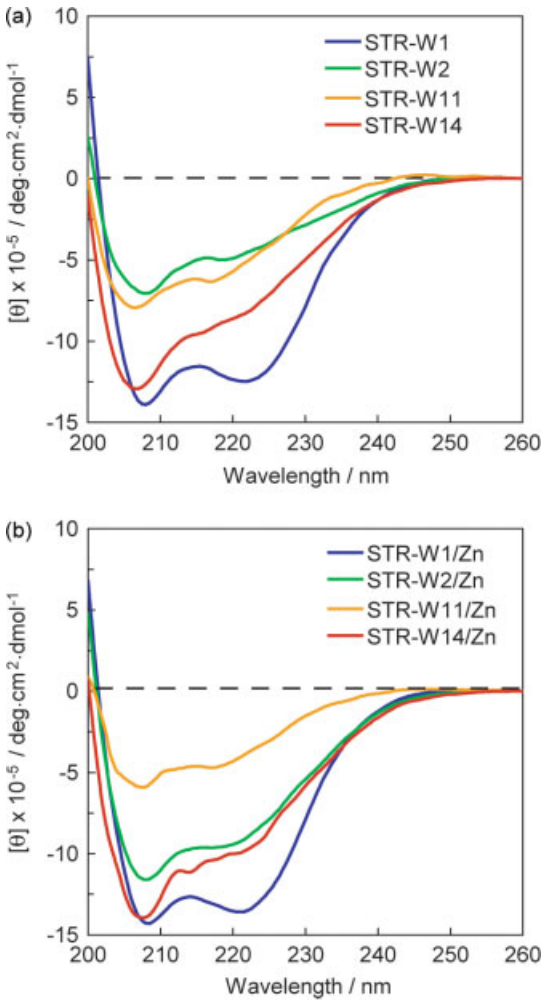

Figure 7. CD spectra of (a) peptides and (b) their Zn complexes in aqueous micellar solution (100 μM peptide, 100 μM $Zn(ClO_4)_2$, 10 mM CTAC, pH 7). Blue, green, yellow, and red line indicates STR-W1, STR-W2, STR-W11, and STR-W14, respectively.

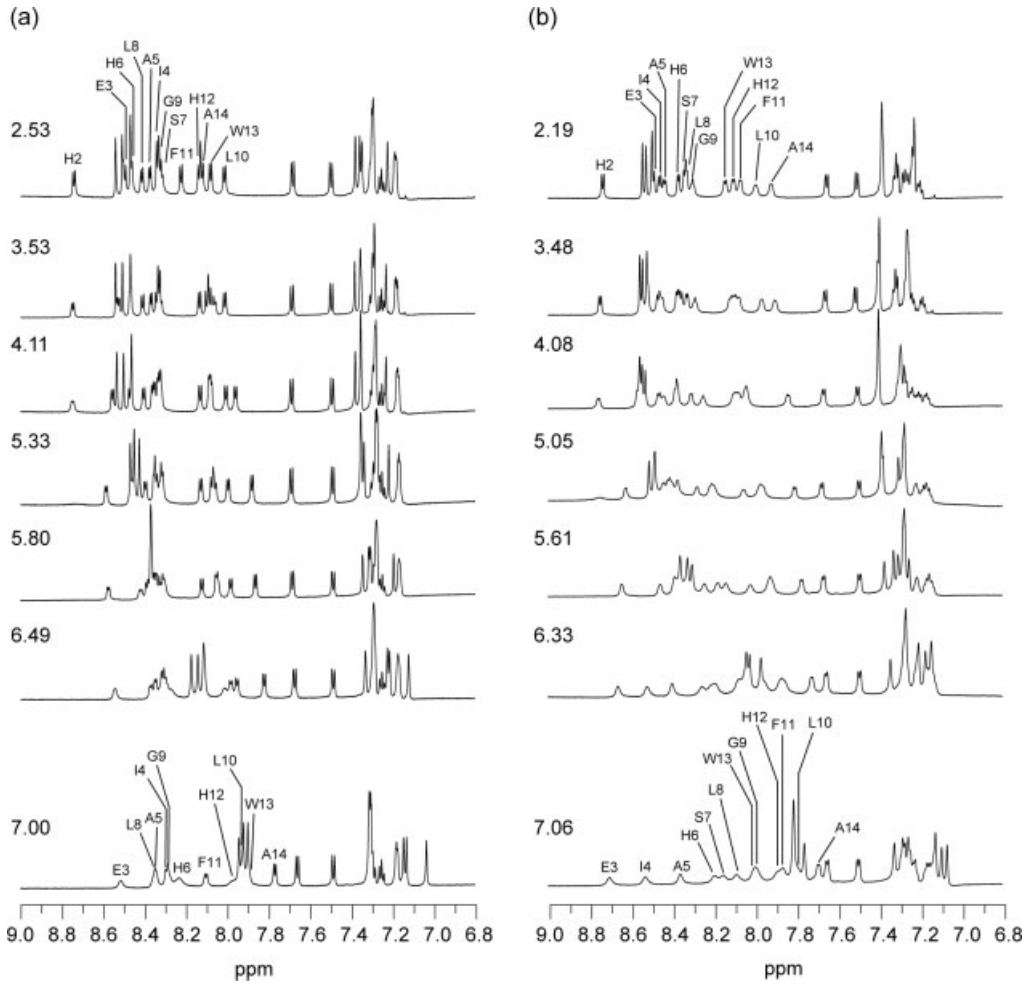

Figure 8. pH-dependent ^{1}H NMR spectra of STR-W14 in (a) aqueous and (b) aqueous CTAB solutions. 1 mM peptide, 25 mM CTAB-d_{33}, 10% D_2O/90% H_2O, 298 K. The pH for each spectrum is shown in the figure.

pH Dependence of Peptide Conformation

The pH dependences of peptide conformation and incorporation into the micelles were investigated by ^{1}H NMR measurements. Although the series of motif fragments with Trp residues, STR-W1, STR-W2, STR-W11, and STR-W14, were incorporated in the micelle, successful helix formation depended on the position of Trp. The incorporation of hydrophobic Trp residue into the motif peptides affected the peptide nature. From the CD analyses of the four peptides, it was found that STR-W1 and STR-W14 exhibited a strong negative cotton effect at 222 nm, indicating that these peptides have helical structures in both the Zn-free and bound forms (Figure 7); on the other hand, the two peptides STR-W2 and STR-W13 exhibited unfolded propensity. Therefore, we analyzed the motif peptide STR-W14, which had the potential for helical folding in the micellar solution. Figure 8(a) and (b) show the ^{1}H NMR spectra of STR-W14 performed in 90% H_2O/10% D_2O in the presence and absence of cetyltrimetylammonium bromide (CTAB-d_{33}, 25 mM) (A CD experiment revealed that the helical conformation is preserved in the concentration range of 25–100 mM.). The proton resonance lines of the peptide in these solutions were assigned by following the conventional strategy of spin-system assembly and sequential assignment using standard homonuclear 2D NMR spectra [24]. Unfortunately, we could not obtain clear signals sufficient for assignment and detailed discussion of the structure for STR-W14/Zn^{2+} in a micellar solution; we instead focused on the apo conformation of STR-W14. As shown in Figure 8, the NH signals of STR-W14 in the micellar solutions were different from those observed in the simple aqueous solution at neutral pH, indicating that the peptide was buried in the micelles. Each NH signal was observed separately in the wide range of the NH region, suggesting the characteristic helix formation. In the acidic pH region, the signal patterns of NHs of the two solutions were almost identical to each other. This is probably because peptide fragments are positively charged in acidic pH and are not incorporated into the cationic CTAB micelles.

The pH-dependent conformational changes of STR-W14 and STR-W14/Zn^{2+} were also studied by CD measurement in the presence and absence of micelles. The results are shown in Figure 9. In an aqueous solution, STR-W14 produces a random coil structure in all pH regions (Figure 9(a)). STR-W14/Zn^{2+} was not only perfectly soluble in the aqueous solution but also had no distinct conformational feature (data not shown). Figures 9(b) and (c) show that the intensities of the negative peaks at 222 and 209 nm increased with increasing the pH of both STR-W14 and STR-W14/Zn^{2+} in the micellar solution. The results suggest that both the peptide and its Zn^{2+} complex have helical conformation in the CTAC micelle in the basic pH region. Such a marked negative extremum at 222 nm was not observed in the absence of CTAC.

Journal of PeptideScience

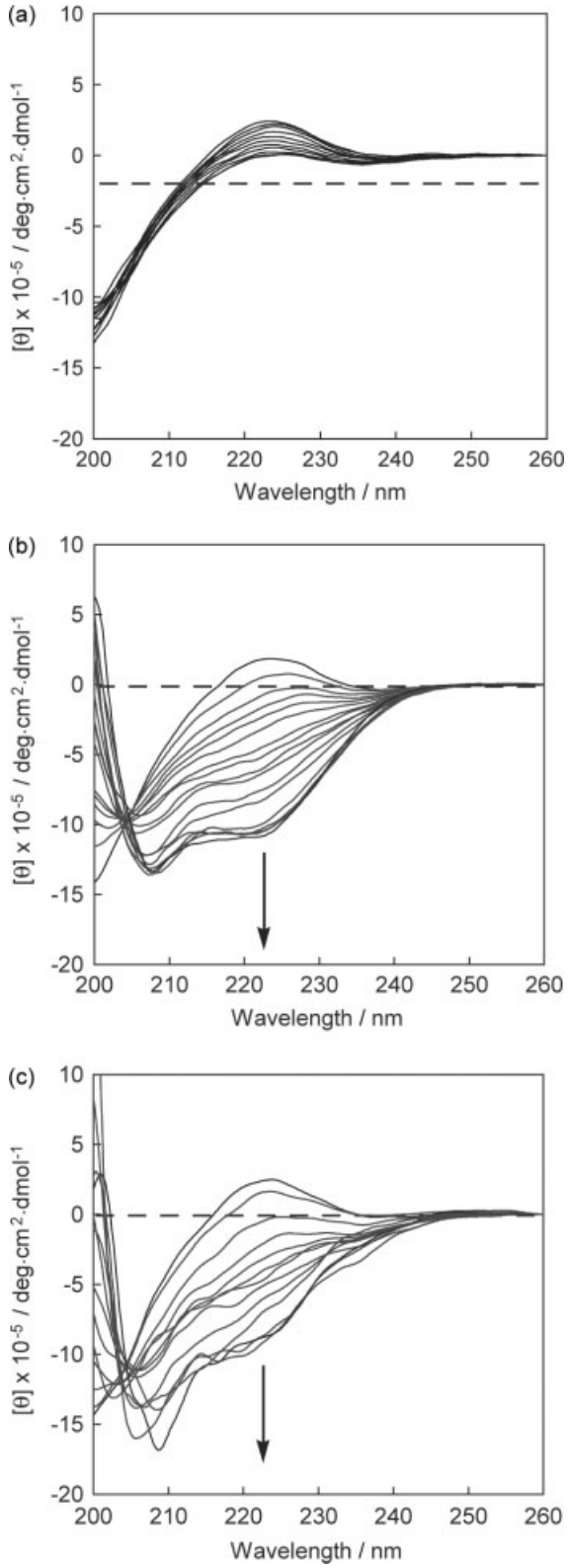

Figure 9. pH-dependent CD spectra of (a) STR-W14 in aqueous solution, (b) STR-W14 in CTAC micellar solution, and (c) STR-W14/Zn^{2+} in CTAC micellar solution; 100 μM peptide, 100 μM $Zn(ClO_4)_2$, 10 mM CTAC solution. pH was adjusted from 3.0 to 10.0 with 0.5 increment; ((a) 3.03, 3.53, 4.04, 4.55, 5.07, 5.53, 6.02, 6.48, 7.10, 7.51, 8.09, 8.58, 9.08, 9.50, 10.01, 10.53, 11.03, 11.53. (b) 3.03, 3.55, 4.05, 4.57, 5.00, 5.47, 6.10, 6.60, 6.99, 7.49, 8.07, 8.58, 9.00, 9.52, 10.02, 10.60, 11.06, 11.59. (c) 2.99, 3.53, 4.04, 4.58, 5.06, 5.51, 6.00, 6.56, 7.01, 7.54, 8.08, 8.58, 9.05, 9.58, 9.99, 10.58, 10.96, 11.58.).

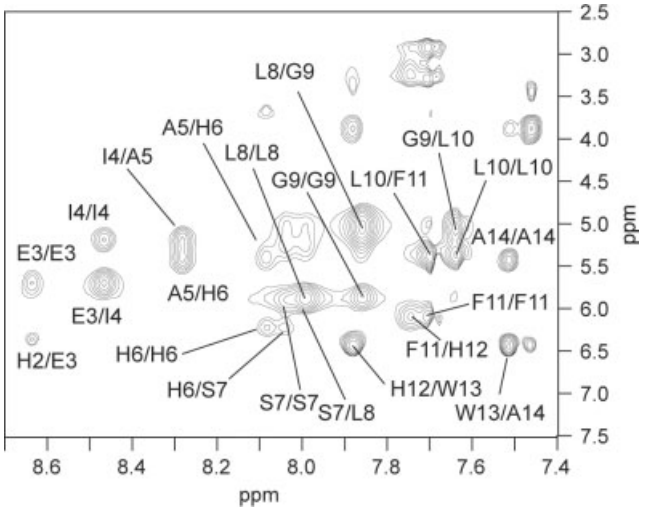

Figure 10. Selected region of NOESY spectra of STR-W14 in aqueous CTAB-d_{42} solution; 2 mM peptide, 50 mM CTAB-d_{42}, 10% D_2O/90% H_2O, pH 7.0, 298 K.

The spectral changes indicate that the conformation of STR-W14 changes from a random coil to a helix with increasing pH in the presence and absence of the micelle. The decreased helicity of STR-W14/Zn^{2+} seems to reveal that Zn^{2+} coordination perturbs the helical structure found in the apo peptide.

NMR Structure

Detailed structural analyses of STR-W14 in the micellar solution by NMR revealed that the peptide has a helical conformation. The NOE correlation for STR-W14 was successfully observed in a solution containing 2 mM STR-W14 and 50 mM CTAB-d_{42} excluding the His2 NH signals (Figure 10). STR-W1 had two conformations in the micellar environment, and structural analyses could not be performed because of the overlapped signals. The three-dimensional structure of STR-W14 was calculated from its NOE data using the simulated annealing method [25] with XPLOR. The 20 lowest energy structures from one hundred generated structures were divided into two conformational families that differed in the folding of three *N*-terminus residues: Ala1, His2, and Glu3 (Figure 11(a) and (b)). The rmsd of the backbone atoms in the following region (4–14) was 0.13, indicating that the two families were practically identical in this region. The NMR structural analyses clarified that the residues in 4–14 formed a rigid helical structure, as suggested by CD measurements, and that the *N*-terminus of STR-W14 was flexible in the micellar solution.

The difference in conformation between the apo state in the micelle and the reported Zn-bound state of stromelysin-1 in the crystal structures is shown in Figure 12. A remarkable difference was found in the *C*-terminus GXXH region. In the Zn-bound state, the *N*-terminus helix ends at Gly8, whose NH is hydrogen-bonded with Gly4 C═O; the following Leu9 NH directs to C═O of Gly4 as well. Leu9 C═O interacts with imidazole NH of His5, and His 12 coordinates to Zn^{2+} to form a loop structure. However, in our apo motif fragment, Gly8 NH was hydrogen-bonded with His5 C═O, and Leu9 NH was with Leu7 C═O; this caused the *C*-terminus part involved in the helix to form an extended helical structure. This helical conformation forces the three His residues to position themselves separately each other. The construction of the hydrogen bonding interactions within the GXXH region seems

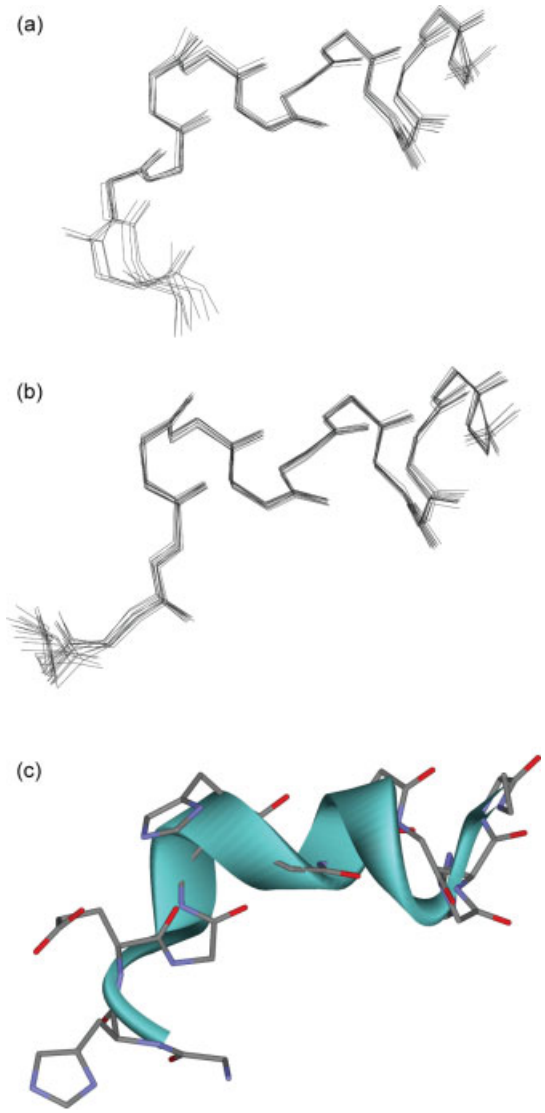

Figure 11. Superpositions of the backbone atoms of (a) the 9 structures (family 1) and (b) the 11 structures (family 2). (c) Lowest energy structure from family 1 in ribbon representation. Only side chain atoms of three His and Glu residues are shown for clarity.

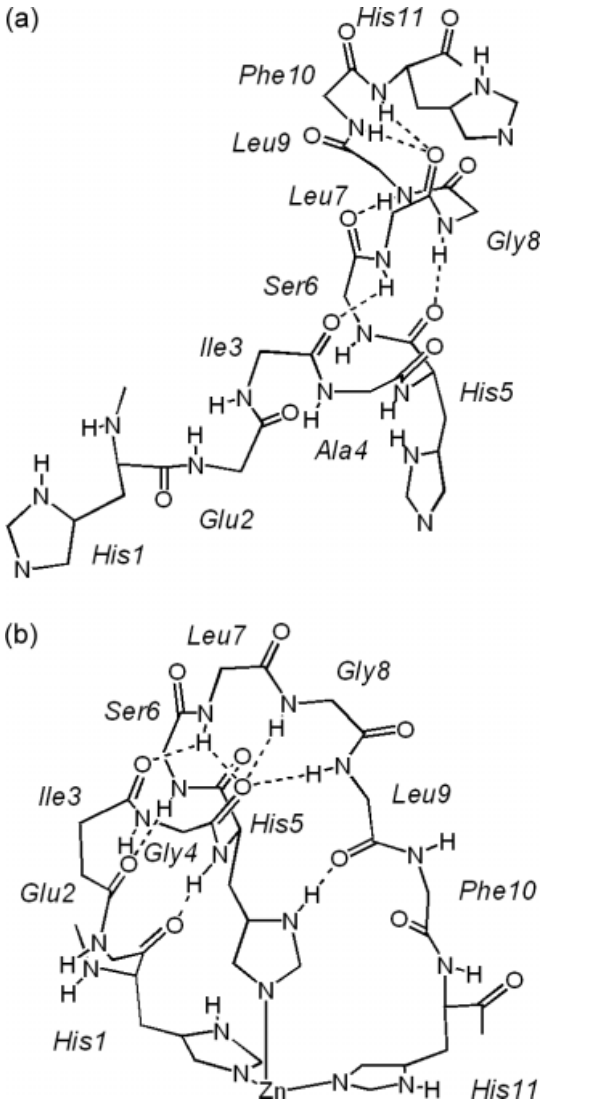

Figure 12. Conformation of the conserved motif, HEXXHXXGXXH, (a) in the apo state in the micellar solution and (b) in zinc-bound state found in the crystal structure. Numbering in the figure starts from His in the motif and the hydrogen bonding is shown in dotted lines.

to result in the key difference that defines the whole conformation as an extended helix or helix-loop.

The structural analyses of the qualitative Zn-binding properties for this motif peptide provide us with an interesting Zn-binding mechanism. The ESI MS experiments indicated that the motif fragment exhibited superior complexation to Zn^{2+} in the hydrophobic environment served by the micelle. The NMR structural analyses of STR-W14 in the aqueous micellar solution revealed that the peptide gives the helical conformation and that the rearrangement of the hydrogen bonding interactions in the GXXH region seemingly enables to change this conformation to the helix-loop structure in the Zn-binding form. Therefore, these results reveal that the motif fragment in this study gives preorganized conformation in hydrophobic circumstances, which facilitates Zn binding. Previous studies using a Zn-binding motif in Zn finger proteins concluded that Zn-binding results in protein folding and enhanced rigidity [6]. For cases at the other extreme, the proteins were completely folded even in the absence of metal [26]. Actually, the motif fragment is almost preserved even in Zn^{2+}-removed astacin [27]. We found that the minimum consensus motif in the metzincin clan, basic Zn-binding motif with extended GXXH region, has the potential to serve as a preorganized Zn-binding scaffold in a hydrophobic environment (Figure 13). This preorganized conformation is different from those observed in the native proteins. The motif structure of the metzincin clan described above is probably promoted not only by the internal force field inherent in the motif but also by forces from other parts of the sequence surrounding the motif.

Conclusion

We analyzed the structural properties of the minimal motif peptide containing HEXXHXXGXXH, which is highly conserved in the metzincin clan of Zn endopeptidases, in the hydrophobic environment of micellar solutions. Our structural investigation indicated that this consensus motif peptide inherently folds into

Journal of PeptideScience

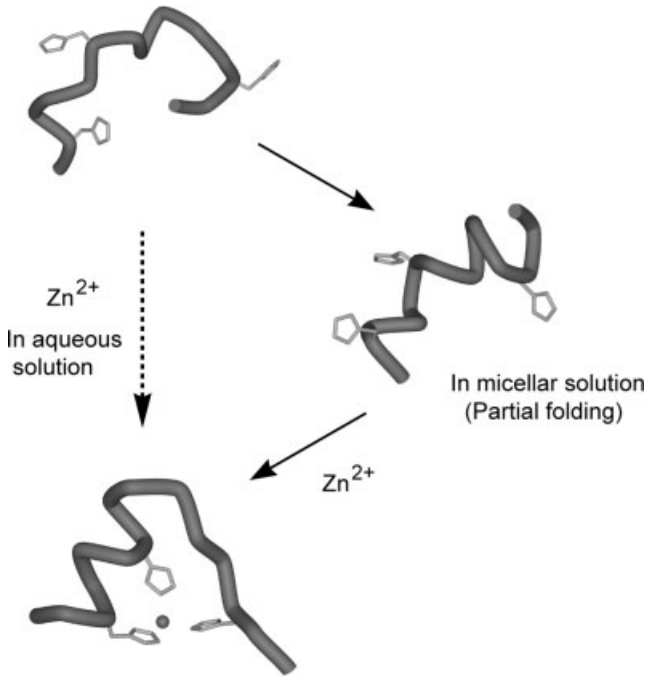

Figure 13. Schematic representation of zinc-binding behavior of the motif peptide in the hydrophobic environment.

a helix-containing conformation in hydrophobic circumstances. Although the incorporation of hydrophobic Trp residue into the motif peptides presumably affects the peptide nature, the two peptides, STR-W1 and STR-W14, exhibited successful helical folding in the hydrophobic area of the cetyltrimethylammonium chloride micelle; the other two, STR-W2 and STR-W13, did not fold sufficiently. We evaluated hydrophobicity using Trp fluorescence. The steady-state fluorescence and quenching experiments clearly suggested that the peptides are incorporated into micelles. The CD and NMR measurements led to the conclusion that the minimal motif fragment folds into a helix in the hydrophobic environment of aqueous micellar solutions, and we found that the preorganized helix-containing conformation promotes the successful binding of Zn^{2+}. Our systematic investigation on the minimal motif peptides provides basic information for understanding their properties with regard to Zn binding and peptide folding.

Experimental

Materials

Boc–Ala–Pam resin and Boc amino acids were purchased from Nova BioChem. All solvents were distilled over appropriate drying agents and degassed prior to use. CTAC and polyethyleneglycol lauryl ether Briji35 were purchased from Aldrich. DPC was purchased from Acros Chemical. SDS was purchased from Kanto Chemicals. Acrylamide for quenching experiments was purchased from Wako Chemicals. NaOD and DCl for NMR titration experiments were purchased from Aldrich. CTAB-d_{33} and CTAB-d_{42} were purchased from C/D/N Isotopes Inc.

Solid Phase Peptide Synthesis

All peptides were synthesized manually by standard solid phase methods using Boc chemistry with benzotriazole-1-yl-oxy-tris-pyrrolidino-phosphonium hexafluorophosphate (PyBOP)/HOBt activation. Preloaded PAM resin was used to synthesize the peptides used in this study. Deprotected peptides were cleaved from the resin by treatment with a cooled solution of TFA/thioanisole/*m*-cresol/ethanedithiol (62 : 18 : 11 : 9) and followed by TMSOTf. The mixed solution was kept at 0 °C for 3 h. The filtrate was dispersed in cold ether, and precipitated peptides were washed with ether and dried. The peptides were dissolved in an aqueous solution, and the solution pH was adjusted to 8 with triethylamine. The solution was mixed with 1 M NH_4F at 0 °C, stirred for 30 min, and concentrated. The residues obtained from the concentration were purified using a Sep-Pak vac 3 cc + C18 cartridge and a C18 reverse phase HPLC column with an acetonitrile gradient containing 0.05% TFA. The purity of all peptides was greater than 99.6%, as determined by HPLC. All peptides were characterized by MALDI-TOF MS.

Peptide Micellar Solution

In this study, the incorporation of model peptides into micelles was performed by a previously reported procedure with some modifications [28]. We also studied the method for the complex formation of these peptides with Zn^{2+} in the presence and absence of surfactants in several organic solvents. Peptides with $Zn(ClO_4)_2 \cdot 6(H_2O)$ were mixed with a surfactant in DMSO, and the obtained solution was freeze-dried and dissolved in an aqueous buffer solution. From this study, we found that DMSO increases the helix content of the peptides in the micellar solution.

Physical Measurements

UV-vis spectra were recorded on a Shimadzu spectrophotometer (UV2200A). MALDI-TOF MS experiments were performed using PerSpective Biosystems Voyager LinerRD VDA-500. ESI-TOF MS was performed using Bruker microTOF. CD spectra were measured on a Jasco J-810. The %(Helix) was calculated from $[\theta]_{222}$ based on an ellipticity value of −36 000 for 100% α-helical content; this was derived from the equation $X_H{}^n = X_H{}^\infty(1 - k/n)$, where $X_H{}^\infty$ is −37 400, the wavelength dependent constant k is 2.5, and n is the number of helical residues [29].

Fluorescence Spectroscopy

Fluorescence spectra were recorded on a Shimadzu fluorescence spectrophotometer (RF5300-PC) with emission and excitation slits width of 5 nm. The excitation wavelength was 280 nm, and emission spectra were recorded from 300 to 450 nm. The scan rate was 60 nm/s. The concentration of the peptides and Zn^{2+} was 15 μM. The micelle concentration was 10 mM.

Acrylamide quenching experiments were carried out at an excitation wavelength of 290 nm to reduce the absorbance of acrylamide. An acrylamide stock solution (1 M) was added to the sample in the presence and absence of series of micelles.

The data were analyzed using the Stern–Volmer equation:

$$F_0/F = 1 + K_{SV} \cdot [Q],$$

where F_0 is the fluorescence intensity at zero quencher concentration, F is the fluorescence intensity at any given quencher concentration, and K_{SV} represents the apparent Stern–Volmer quenching constant obtained from the slope of the F_0/F *versus* [Q] plot.

Table 2. Restraints and Structural Statistics for NMR structures

distance restraints	176	
intraresidue	75	
sequential, $\|i-j\|=1$	56	
medium range, $1<\|i-j\|\leq 4$	5	
NOE violations > 0.4 Å	0	
statistics for structural calculations		
family 1 (9 structures)		
rmsd from idealized covalent geometry		
bonds (Å)	0.0051 ± 0.0001	
angles (deg)	0.8368 ± 0.0115	
improper (deg)	0.6809 ± 0.0201	
rmsd from experimental data		
NOEs (Å)	0.0763 ± 0.0007	
Average ensemble rmsd (Å)	backbone atoms	heavy atoms
	0.30	1.06
family 2 (11 structures)		
rmsd from idealized covalent geometry		
bonds (Å)	0.0052 ± 0.0001	
angles (deg)	0.8425 ± 0.0092	
improper (deg)	0.6788 ± 0.0150	
rmsd from experimental data		
NOEs (Å)	0.0756 ± 0.0007	
Average ensemble rmsd (Å)	backbone atoms	heavy atoms
	0.19	1.01
Ramachandran analysis (%)[a]		
residues in most favored regions	68.5	
residues in additional allowed regions	25.9	
residues in generously allowed regions	4.6	
residues in disallowed regions	1.0	

[a] Generated using PROCHECK-NMR on the ensemble of the 20 lowest-energy structures

NMR Experiments and Molecular Modeling

The ^{1}H NMR spectra were acquired on a Bruker AVANCE 600 MHz spectrometer. All complete proton resonance assignments were performed in the DQF-COSY, TOCSY, [30,31] and NOESY experiments. These spectra were recorded with a 7788.2 Hz spectral width in both dimensions; there were 2048 data points in $f2$ and 512 data points in $f1$ with 16 scans at each increment.

All data were processed with a NMR Pipe and analyzed with PIPP software. Inter-proton distances were derived from mononuclear 2D NOESY spectra recorded with a mixing time (τ_m) of 100 ms. Appropriate values for the pseudo atoms were added to the distance using methyl protons and non-stereospecifically assigned methylene protons. The NOEs were characterized on the basis of the total volumes of the cross-peaks. The upper bounds for the NOE constraints were calibrated using known ^{1}H(β)–^{1}H(β') and sequential ^{1}H–^{1}H distances. The lower distance limit was considered as the sum of the van der Waals radii for the two hydrogen atoms (1.8 Å).

The three-dimensional structure of the peptide was calculated from the experimental constraints using the simulated annealing method with XPLOR (version 3.851) [32]. The calculation was performed according to a similar procedure described previously. [33,34] The structures and structural parameters were analyzed using PROCHECK-NMR (Table 2) [35].

Acknowledgement

This work was supported by a Grant-in-Aid for Scientific Research No. 13640565 from the Ministry of Education, Culture, Sports, Science, and Technology (MEXT) of the Japanese Government.

Supporting information

Supporting information may be found in the online version of this article.

References

1 Ueyama N, Terakawa T, Nakata M, Nakamura A. Positive shift of redox potential of [F4S4(Z-cys-Gly-Ala-OMe)4]2- in Dichloromethane. *J. Am. Chem. Soc.* 1986; **105**: 7098–7102.
2 Yamamura T, Wataneb T, Kikuchi A, Yamane T, Ushiyama M, Hirota H. Conformation control of peptides by metal ions. Coordination conformation correlation observed in a model for Cys-X-Y-Cys/M2+ in Proteins. *Inorg. Chem.* 1997; **36**: 4849–4859.
3 Kim C, Berg JM. A 2.2 A resolution crystal structure of a designed zinc finger protein bound to DNA. *Nature Struct. Biol.* 1996; **3**: 940–945.
4 Guerrerio AL, Berg JM. Metal ion affinities of the zinc finger domains of the metal responsive element-binding transcription factor-1 (MTF-1). *Biochemistry* 2004; **43**: 5437–5444.
5 Laity JH. Cys2His2 zinc finger proteins. In *Handbook of Metalloproteins*, Vol. 3, Messerschmidt A, Bode W, Cygler M (eds.). John Wiley & Sons: Chichester, 2001; 307–323.
6 Berg JM, Godwin HA. Lessons from zinc-binding peptides. *Annu. Rev. Biophys. Biomol. Struct.* 1997; **26**: 357–371.
7 Cox EH, McLendon GL. Zinc-dependent protein folding. *Curr. Opin. Chem. Biol.* 2000; **4**: 162–165.
8 Vallee BL, Auld DS. Zinc coordination, function and structure of zinc enzymes and other proteins. *Biochemistry* 1990; **29**: 5647–5659.
9 Rawlings ND, Barrett AJ. Evolutionary families of peptidases. *Biochem. J.* 1993; **290**: 205–218.
10 Matthews BW. Structural basis of the action of thermolysin and related zinc peptidases. *Acc. Chem. Res.* 1988; **21**: 333–340.
11 Stöcker W, Grams F, Baumann U, Reinermer P, Gomis-Rüth FX, McKay DB, Bode W. The metzincins – topological and sequenctial relations between the astacins, adamalysins, serralysins, and matrixins (collagenases) define a superfamily of zinc-peptidases. *Protein Sci.* 1995; **4**: 823–840.
12 Lipscomb WN, Strater N. Recent advances in zinc enzymology. *Chem. Rev.* 1996; **96**: 2375–2433.
13 Bode W, Gomis-Rüth FX, Stöcker W. Astasis, serralysins, snake venom and matrix metalloproteinases exhibit identical zinc-binding environments (HEXXHXXGXXH and Met-turn) and topologies and should be grouped into a common family, the 'metzincins'. *FEBS lett.* 1993; **331**: 134–140.
14 Stöcker W, Bode W. Structural features of a super family of zinc-endopeptidases: the metzincins. *Curr. Opin. Struct. Biol.* 1995; **5**: 383–390.
15 Ishizuka H, Abe M, Tamura K, Onoda A, Yamamura T. *Peptide Sci.* 2003; **40**: 433–434.
16 Raussens V, Slupsky CM, Sykes BD, Ryan RO. Lipid-bound structure of an apolipoprotein E-derived peptide. *J. Biol. Chem.* 2003; **278**: 25998–26006.
17 Tinoco LW, da Silva JA, Leite A, Valente AP, Almeida FCL. NMR structure of PW2 bound to SDS micelles. A Tryptophan-rich anticoccidial peptide selected from phase display libraries. *J. Biol. Chem.* 2002; **277**: 36351–36356.
18 Neidigh JW, Andersen NH. Peptide conformational changes induced by tryptophan-phosphocholine interactions in a micelle. *Biopolymers* 2002; **65**: 354–361.

19 Oren Z, Ramesh J, Avrahami D, Suryaprakash N, Shai Y, Jelinek R. Structure and mode of membrane interaction of a short a helical lytic peptide and its diastereomer determined by NMR, FTIR, and fluorescence spectroscopy. *Eur. J. Biochem.* 2002; **269**: 3869–3880.
20 Park K, Oh D, Shin SY, Hahm K-S, Kim Y. Structural studies of porcine myeloid antibacterial peptide PMAP-23 and its analogues in DPC micelles by NMR spectroscopy. *Biochem. Biophys. Res. Commun.* 2002; **290**: 204–212.
21 Schibli DJ, Hwang PM, Vogel HJ. Structure of the anitimicrobial peptide tritrpticin bound to micelles: a distinct membrane-bound peptide fold. *Biochemistry* 1999; **38**: 16749–16755.
22 Prevelige JP, Fasman GD. Chou-Fasman prediction of the secondary structure of proteins. In *Prediction of Protein Structure and the Principles of Protein Conformation*, Fasman GD (ed.). Plenum Press.: New York, 1989.
23 de Kroon AIPM, Soekarjo MW, de Gier J, de Kruijff B. The role of charge and hydrophobicity in peptide-lipid interaction: a comparative study based on tryptophan fluorescence measurements combined with the use of aqueous and hydrophobic quenchers. *Biochemistry* 1990; **29**: 8229–8240.
24 Wütrich K. *NMR of Proteins and Nucleic Acids*. John Wiley & Sons: New York, 1986.
25 Harvel TF. An evaluation of computational strategies for use in the determination of protein structure from distance constraints obtained by nuclear magnetic resonance. *Prog. Biophys. Mol. Biol.* 1991; **56**: 43–78.
26 Nar H, Messerschmidt A, Huber R, van de Kamp M, Cangers GW. Crystal structure of *Pseudomonas aeoruginosa* apo-azurin at 1.85 A. *FEBS Lett.* 1992; **2**: 119–124.
27 Gomis-Rüth FX, Stöcker W, Huber R, Zwilling R, Bode W. Refined 1.8 ang. X-ray crystal structure of astacin, a zinc-endopeptidase from the crayfish *Astacus astacus* L. Structure determination, refinement, molecular structure and comparison with thermolysin. *J. Mol. Biol.* 1993; **229**: 945–968.
28 Liu L-P, Li S-C, Goto NK, Deber CM. Thresholed hydrophobicity dictates helical conformations of peptides in membrane environments. *Biopolymers* 1996; **39**: 465–470.
29 Chen Y-H, Yang JT, Chau KH. Determination of the helix and b form of proteins in aqueous solution by circular dichroism. *Biochemistry* 1974; **13**: 3350–3359.
30 Braunschweiler L, Ernst RR. Coherence transfer by isotropic mixing: application to proton correlation spectroscopy. *J. Magn. Reson.* 1983; **53**: 521–528.
31 Bax A, Davis DG. MLEV-17-based two-dimensional homonuclear magnetization transfer spectroscopy. *J. Magn. Reson.* 1985; **65**: 355–360.
32 Brunger AT. *XPLOR version 3.1, A System for X-ray Crystallography and NMR*. Yale University Press: New Haven, CT, 1998.
33 Onoda A, Yamamoto H, Yamada Y, Lee K, Adachi S, Okamura T-A, Yoshizawa-Kumagaye K, Nakajima K, Kawakami T, Aimoto S, Ueyama N. Switching of turn conformation in an aspartate anion peptide fragment by NH· · ·O- hydorogen bonds. *Biopolymers* 2005; **80**: 233–248.
34 Onoda A, Arai N, Shimazu N, Yamamoto H, Yamamura T. Calcium ion responsive DNA binding in a zinc finger fusion protein. *J. Am. Chem. Soc.* 2005; **127**: 16535–16540.
35 Laskowski RA, Rullmann JA, MacArthur MW, Kaptein R, Thornton JM. AQUA and PROCHECK-NMR: Programs for checking the quality of protein structures solved by NMR. *J. Biomol. NMR* 1996; **8**: 477–486.

